ADVANCED THERAPEUTICS
www.advtherap.com

High-Density Lipoprotein Engineering for Eye-Drop Treatment of Age-Related Macular Degeneration

*Ryosuke Fukuda, Nargis Mahmuda, Sawangrat Kasirawat, Ryo Kawakami, Rumina Shima, Yu Mizukami, Shiori Shibukawa, Yuki Tada, Fumitake Kawanishi, Masatsune Ogura, Kota Matsuki, Yoshinori Nagai, Eri Nakano, Kenji Suda, Akitaka Tsujikawa, and Tatsuya Murakami**

Eye-drop treatments of age-related macular degeneration (AMD) are desirable; however, no clinically approved eye drop has been reported to date. This study aim to evaluate the therapeutic activity of eye-drop instillation of a high-density lipoprotein (HDL) variant bearing a cell-penetrating peptide and neovasculature-targeted peptide (AsnGlyArg [NGR] peptide) in a mouse model at a dose of 0.6–0.85 μg protein/eye drop. The results reveal that the activity of the abovementioned variant was >10-fold higher than that of the previous variant lacking an NGR peptide. In addition, the anti-inflammatory activity, cholesterol-efflux capacity, and antiangiogenic activity of reconstituted HDL are significantly augmented by the attachment of these two peptides. The mechanism underlying this dramatic improvement is likely the expression of CD13, an NGR peptide receptor, on the cornea and conjunctiva in mice. CD13 mRNA/protein expression is also detected in cultured human corneal and conjunctival cells. These results demonstrate that NGR peptide is an unprecedented class of an absorption enhancer on the eye surface. Thus, HDL engineering is a potential strategy for developing eye drops to treat neovascular AMD by enhancing the ocular surface absorption and HDL functionalities.

1. Introduction

Eye-drop instillation is the least invasive therapy for eye diseases. Many eye-drop formulations have been developed to increase their therapeutic efficacy by prolonging their eye-surface retention and/or enhancing their absorption. Regarding these formulations, various in situ gelling systems are available in clinical settings for prolonging their eye-surface retention;[1] however, no "active" system has been clinically approved for enhancing their absorption to date. The additional absorption-enhancing abilities of clinically approved additives, such as benzalkonium chloride (preservative), cyclodextrin (solubilizer), and ethylenediamine-*N,N,N′,N′*-tetraacetic acid (stabilizer), as well as Lacrimera (Lacrimera is a trademark of Croma-Pharma) have been reported in the management of dry-eye diseases.[2] However, there is a lack of clinically effective eye-drop formulations for treating posterior-eye diseases whose

R. Fukuda, N. Mahmuda, S. Kasirawat, R. Kawakami, R. Shima, Y. Mizukami, S. Shibukawa, Y. Tada, F. Kawanishi, Y. Nagai, T. Murakami
Department of Biotechnology and Pharmaceutical Engineering
Graduate School of Engineering
Toyama Prefectural University
Imizu, Toyama 939-0398, Japan
E-mail: murakami@pu-toyama.ac.jp

N. Mahmuda
Department of Pharmacy
Dhaka International University, Badda
Dhaka 1212, Bangladesh

S. Kasirawat
Department of Pharmaceutical Sciences
Faculty of Pharmacy
Chiang Mai University
Chiang Mai 50200, Thailand

M. Ogura
Department of General Medical Science
Chiba University Graduate School of Medicine
Chiba, Chiba 260–8677, Japan

K. Matsuki
Hirosaki University Graduate School of Medicine
Hirosaki, Aomori 036–8562, Japan

E. Nakano, K. Suda, A. Tsujikawa
Kyoto University Graduate School of Medicine
Sakyo-ku, Kyoto 606–8507, Japan

T. Murakami
Institute for Integrated Cell-Material Sciences (iCeMS)
Kyoto University
Sakyo-ku, Kyoto 606–8501, Japan

The ORCID identification number(s) for the author(s) of this article can be found under https://doi.org/10.1002/adtp.202300186

DOI: 10.1002/adtp.202300186

lesion sites are away from the eye surface. In this regard, cell-penetrating peptides (CPPs) have recently attracted increasing attention as penetration enhancers.[3] Thus, absorption enhancers with different mechanisms of action can further advance the therapeutic development of eye-drop formulations for posterior-eye diseases.

In developed countries, age-related macular degeneration (AMD) is the leading cause of blindness in older individuals,[4] and its pathogenesis involves choroidal neovascularization, lipid deposition, chronic inflammation, and oxidative stress.[5] The latter three are also observed in atherosclerosis. Currently, the first treatment option for AMD is intravitreal injection of antiangiogenesis proteins, which is associated with high invasiveness and several complications. Therefore, eye drops are desired; however, no clinically approved eye drops have been reported to date.

High-density lipoprotein (HDL) is a nanoparticle with a diameter of ≈10 nm and antiatherogenic properties;[6] its nascent form has been reconstituted with recombinant apolipoprotein A-I and phosphatidylcholine.[7] We previously reported that a library of the engineered nascent forms with different CPPs, phospholipids, and sizes were screened for the efficiency of posterior drug delivery via eye-drop instillation, and the form with the best efficiency provided therapeutic efficacy in a mouse model of neovascular AMD.[8] Importantly, therapeutic efficacy was observed for both drug cargo and HDL variant. This finding suggested that HDL functionalities were beneficial in the mouse model, and HDL may exhibit better efficacy in clinical AMD because of the pathogenic similarities between AMD and atherosclerosis. The variant has a slightly larger diameter of ≈15 nm and contains the sole phospholipid 1,2-distearoyl-*sn*-glycero-3-phosphocholine (DSPC) and the peptide penetratin (PEN) as CPPs, the latter of which was fused to the C-terminus of the protein component. As future HDL variants may not have a disk shape and high density, we designated our variants as engineered lipoproteins (eLPs). We evaluated the efficacy of the abovementioned best (eLP1) eye drop with optimal therapeutic activity in AMD model mice by attaching an active targeting peptide to the neovasculature, i.e., NGR tripeptide,[9] and explored the biological activities of eLP1 and its NGR adduct (eLP2). The latter is important because to the best of our knowledge, the effects of HDL genetic engineering using functional peptides on HDL functionality have not been reported to date. This functionality is beneficial for treating atherosclerosis and possibly AMD that partly share its pathogenesis with atherosclerosis.[5] This study aimed to evaluate the therapeutic activity of eye-drop instillation of eLP2 in a mouse model via absorption enhancement. The therapeutic efficacy of eLP2 was >10-fold higher than that of eLP1 in the AMD mouse model. Thus, we demonstrated that HDL protein engineering is a practical strategy for significantly increasing HDL functionalities.

2. Results

2.1. Preparation and Characterization of CD13-Targeted HDL Variants

The NGR peptide was fused to the N-terminus of the protein moiety of eLP1 via a Gly–Gly linker, which contained the PEN peptide at the C-terminus. We previously regarded DSPC as the best among the three types of phosphatidylcholines bearing two C14:0, C16:0, or C18:0 fatty acids in terms of their posterior cargo delivery efficiency (**Table 1**).[8] The resulting fusion protein of NGR and PEN peptides and DSPC successfully generated 17-nm nanoparticles (eLP2). The discoidal shape of eLP2 was clearly visualized via atomic force microscopy (AFM) analysis (Figure S1, Supporting Information). The circular dichroism (CD) spectra of eLP1, eLP2, and reconstituted HDL lacking NGR/PEN peptides (rHDL) were similar (Figure S2, Supporting Information), suggesting that the effect of NGR fusion on the secondary structure of the protein moiety of eLP1 was negligible. The detailed properties of the three samples are summarized in Table 1.

Table 1. Characterization of the reconstituted lipoprotein nanoparticles used in this study.

	rHDL	eLP1	eLP2
Height (nm)	–	6.2 ± 1.2[a)]	4.6 ± 0.3
Diameter (nm)	17.8 ± 3.7	16.6 ± 1.9	17.0 ± 1.7
Zeta potential (mV)	−8.7 ± 3.1	−3.2 ± 2.3	−5.1 ± 2.2
Lipid-to-protein molar ratio	136 ± 17	139 ± 27	127 ± 41

[a)] Ref. 8. Data are presented as the mean ± standard deviation (N = 3).

2.2. Therapeutic Efficacy of eLP2 Eye Drops in a Mouse Model of Neovascular AMD

The therapeutic efficacy of eLP2 eye drops was assessed in a mouse model of neovascular AMD; e.g., mice with laser-induced choroidal neovascularization (CNV). **Figure 1**A shows immunofluorescence images of CNVs after eye-drop instillation (1.2 μg protein/eye drop; twice daily for 1 week). No apparent damage to the cornea was observed after repeated instillations of eLP2 (data not shown), consistent with our results of various cytotoxicity assays (Figure S3, Supporting Information). The CNV area became smaller in the eLP2 arm than in the eLP1 arm (Figure 1B). Examination of the dose dependency of eLP2 (Figure 1C) revealed that its efficacy plateaued at the dose of 1.2 μg protein/eye drop. Based on the mean values, the minimum saturation dose was estimated to be 0.6–0.85 μg protein/eye drop. In our previous study using eLP1, a dose of 8.7 μg protein/eye drop was utilized, which could not provide such saturated efficacy.[8] These results clearly demonstrate that the therapeutic efficacy of eLP1 in CNV mice was dramatically improved (>10 times) by the NGR peptide fusion.

2.3. Ocular Surface Adhesion of eLP2 in Mice

The CNV-targeting capability of eLP1 after NGR fusion improved by approximately 5-fold (Figure S4A,B, Supporting Information), which was lower than the abovementioned result. The retinal inner layer and choroid regions near the CNV area showed a further smaller difference between eLP1 and eLP2 (Figure S4C–E, Supporting Information). Therefore, we decided to explore mechanisms other than CNV targeting. Regarding eye-drop formulations, the cornea and conjunctiva are the greatest barriers to absorption, which are avoided via intravenous administration. Histochemical analyses of mouse ocular tissue sections were

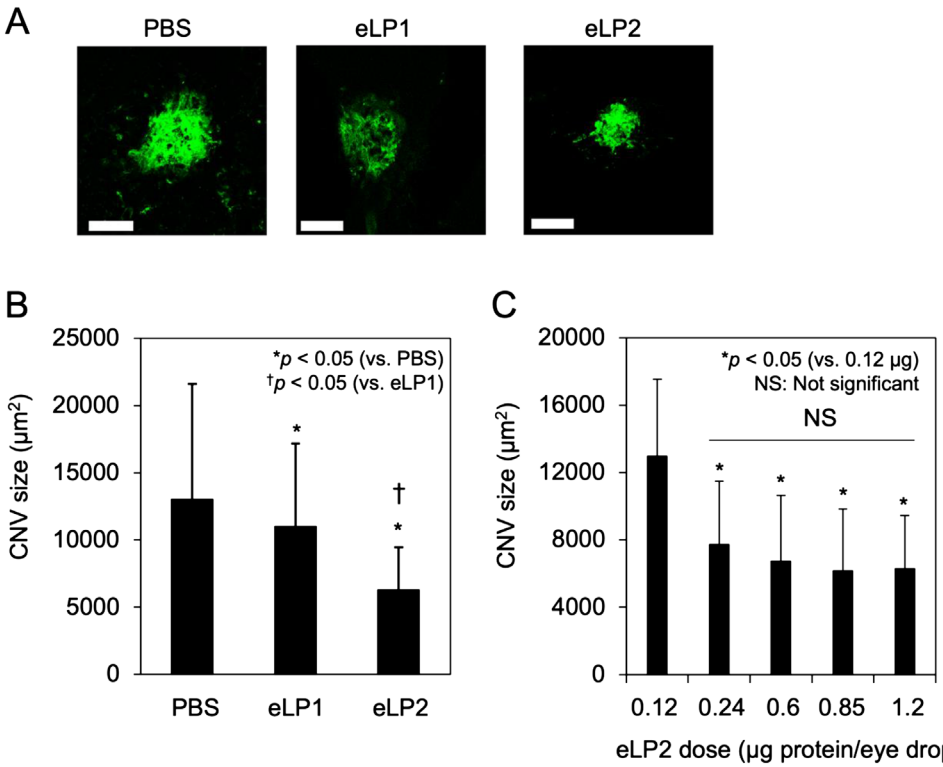

Figure 1. Therapeutic efficacy of engineered lipoprotein 2 (eLP2) eye drops in choroidal neovascularization (CNV) mice. A) Confocal images of the CNV area. B) Quantitative analysis of engineered lipoprotein 1 (eLP1) and eLP2. C) Dose dependency of eLP2. Mouse eyes (N ≥ 6) were enucleated after 1 week of the instillation of phosphate-buffered saline (PBS), eLP1, or eLP2. Data are presented as the mean ± standard deviation. Bar, 100 μm.

initially performed using fluorescently labeled eLP2. At 30 min after eLP2 instillation, a strong fluorescence signal was detected from the cornea (**Figure 2**A), which was much higher than that after eLP1 instillation, and the mean signal value for eLP2 was 5-fold higher than that for eLP1 and 7-fold higher than that for rHDL (Figure 2B, black bar). These results demonstrated that the corneal absorption of eLP2 was significantly enhanced by the NGR peptide fusion. Our histochemical analysis indicated CD13 expression in the cornea and conjunctiva of normal mice (**Figure 3**A). Therefore, the therapeutic efficacy of eLP2 was also associated with the improved absorption, most likely via the interaction of NGR and CD13 on the ocular surface, which may have a positive influence on the improved CNV-targeting capability (Figure S4A,B, Supporting Information).

2.4. Binding of eLP2 in Cultured Human Corneal and Conjunctival Cells

To gain insights into the molecular mechanism underlying the corneal absorption of eLP2, in vitro studies were performed in cultured human corneal epithelial-transformed (HCE-T) and conjunctival (Chang conjunctiva) cells. As shown in Figure 3B and Figure S5 (Supporting Information), CD13 protein and mRNA expression was clearly detected in both cell types; however, its mRNA expression was not detected in cultured human retinal pigment epithelial (ARPE-19) cells. Human umbilical vein endothelial cells (HUVECs), which were used as positive control cells,[10] expressed *CD13* under our experimental conditions. In accordance with the abovementioned in vivo results, eLP2 showed stronger affinity toward all cells than eLP1. Additionally, the effect of NGR fusion on the enhanced affinity was higher in HCE-T and Chang conjunctiva cells than in HUVECs under normal conditions (**Figure 4**). These results indicate that compared with HUVECs, both HCE-T and Chang conjunctiva cells exhibit an enhanced expression of a specific form of CD13, which is recognizable by NGR peptide, because the total CD13 mRNA expression was considerably higher in HUVECs than in the other two cell types.

2.5. HDL Functionalities of eLP2 in HUVECs

Modulation of HDL functionalities responsible for the therapeutic efficacy of eLP2 in CNV mice is considered another mechanism for the result displayed in Figure 1. Thus, the anti-inflammatory activity of eLP2 was initially assessed in HUVECs because endothelial cells become angiogenic during inflammation.[11] The lipopolysaccharide (LPS)-induced interleukin (IL)−1B mRNA expression was dose-dependently inhibited by eLP2, and this inhibition was significantly higher than that for rHDL at 150 μg mL^{-1} but was comparable to that for eLP1 (**Figure 5**A). However, eLP1 and eLP2 themselves did not significantly increase the expression (Figure S6A, Supporting Information). These results suggest that the addition of the PEN peptide contributes to the increased anti-inflammatory activity

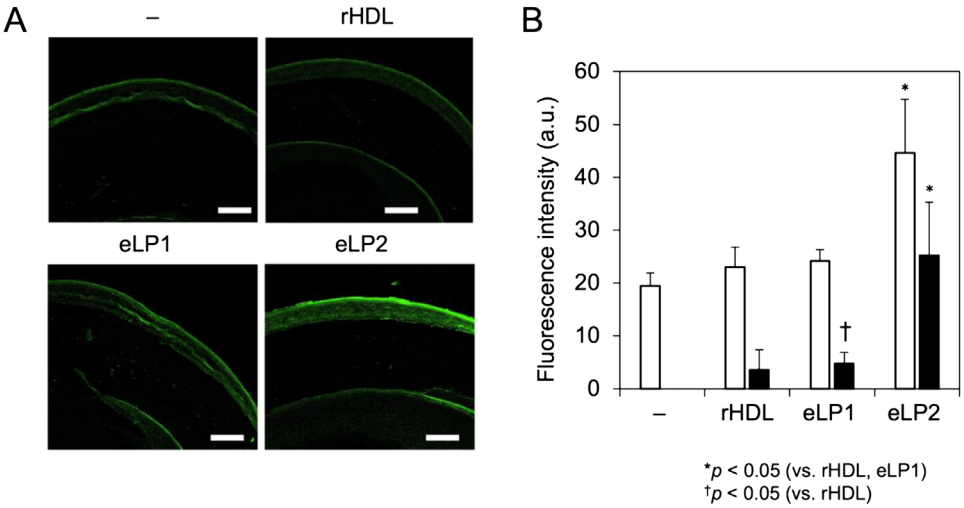

Figure 2. Binding of engineered lipoprotein 2 (eLP2) to the mouse cornea after eye-drop instillation. A) Fluorescence images of the mouse cornea. The green signal for the control (–) indicates the autofluorescence from the mouse tissue. B) Semiquantitative analysis of images in (A) using ImageJ. All intensity data were divided by the area values. The fluorescence signal intensity/area data in (A) (white bar) as well as the data obtained after subtracting the mean background value for the control (black bar) are shown. Mouse eyes (N = 4) were enucleated 30 min after the instillation of phosphate-buffered saline (PBS), or 1,2-dipalmitoyl-*sn*-glycero-3-phosphoethanolamine-*N*-(7-nitro-2-1,3-benzoxadiazol-4-yl) ammonium salt (NBD)-labeled reconstituted high-density lipoprotein lacking penetratin and NGR peptides (rHDL), engineered lipoprotein 1 (eLP1), or engineered lipoprotein 2 (eLP2) (1.5 μM NBD). Data are presented as the mean ± standard deviation (N = 5). Bar, 200 μm.

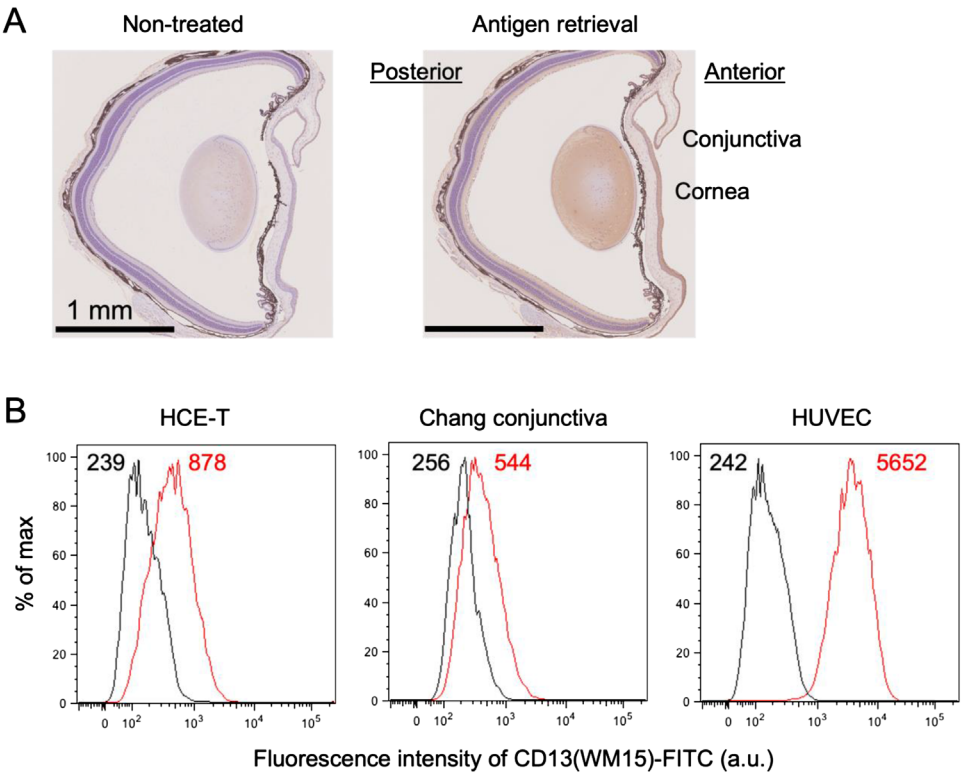

Figure 3. CD13 expression in a normal mouse eye and cultured human cells. A) Immunohistochemical analysis of a normal mouse eye. B) Flow cytometry analysis of cultured human corneal epithelial-transformed (HCE-T) cells, human conjunctival cells (Chang conjunctiva), and human umbilical vein endothelial cells (HUVECs) unstained (black) or stained with fluorescein isothiocyanate (FITC)-labeled anti-CD13 antibody (WM15, 5 μL sample^{-1}) (red). The values in the panels indicate the mean fluorescence intensities.

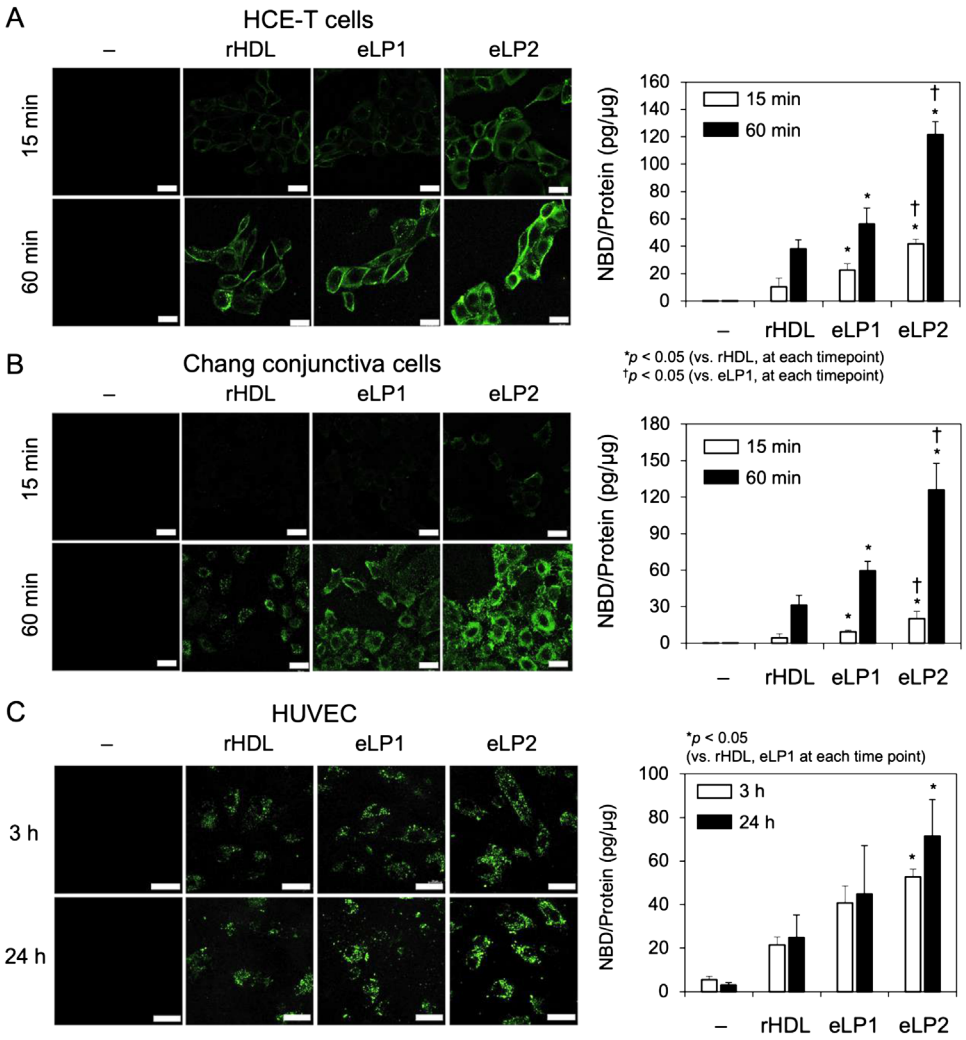

Figure 4. Binding and uptake of engineered lipoprotein 2 (eLP2) in cultured human cells. A) Cultured human corneal epithelial-transformed (HCE-T) cells. B) Chang conjunctiva cells. C) Human umbilical vein endothelial cells (HUVECs). Cells were treated with PBS or 1,2-dipalmitoyl-*sn*-glycero-3-phosphoethanolamine-*N*-(7-nitro-2-1,3-benzoxadiazol-4-yl) ammonium salt (NBD)-labeled reconstituted high-density lipoprotein lacking penetratin and NGR peptides (rHDL), engineered lipoprotein 1 (eLP1), or engineered lipoprotein 2 (eLP2) (1.5 μM NBD). Quantitative data are also shown for each image. Data are presented as the mean ± standard deviation (N = 5). Bar, 40 μm.

of rHDL in LPS-treated HUVECs. This increase is attributed to the intrinsic anti-inflammatory activity of the PEN peptide.[12] In contrast, IL1B mRNA expression was more efficiently inhibited by eLP1 than by a physical mixture of rHDL and PEN peptide (Figure S6B, Supporting Information), clearly highlighting the advantage of the genetic fusion of PEN peptide with rHDL.

The anti-inflammatory activity of eLP2 was further assessed in tumor necrosis factor (TNF)-α-treated HUVECs. Vascular cell adhesion molecule-1 (VCAM-1) protein expression induced by TNF-α was similarly inhibited by rHDL, eLP1, and eLP2, and their activity was significantly higher than that of native HDL from human plasma (nHDL) (Figure 5B,C). In the vascular endothelial growth factor (VEGF)-induced tube formation (angiogenesis) assay, all HDL samples showed significant inhibitory activities, and eLP2 was demonstrated to be a better inhibitor than eLP1 (Figure 5D,E).

2.6. HDL Functionalities of eLP2 in Cultured Human Macrophage Cells (THP-1)

Another cell target of HDL is macrophages. HDL accepts cholesterol molecules that are effluxed from the cells. Compared with nHDL, all reconstituted HDL samples (rHDL, eLP1, and eLP2), which contained DSPC as the only lipid, showed high cholesterol-efflux capacities; eLP1 and eLP2 showed better capacity than rHDL (nHDL < rHDL < eLP1 ≈ eLP2, **Figure 6**A). Then, the anti-inflammatory activity of eLP2 was examined in LPS-treated THP-1 macrophages, in which TNF-α secretion was induced. As shown in Figure 6B, eLP2 dose-dependently suppressed the secretion, and its efficacy was comparable to that of eLP1. In confocal analysis, the binding capacity of eLP1 and eLP2 to THP-1 macrophages was comparable but was considerably higher than that of rHDL (Figure 6C). This comparable binding was

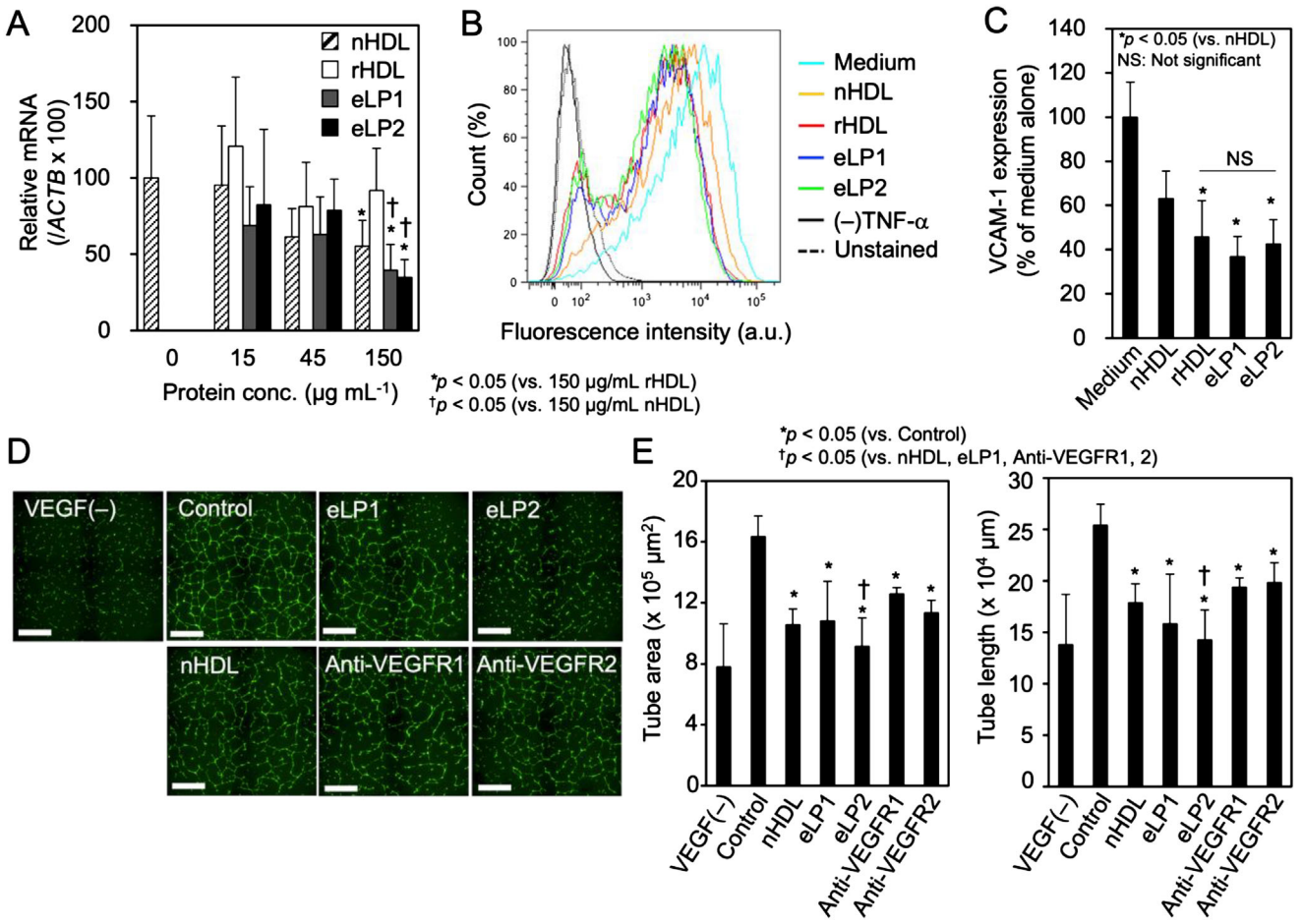

Figure 5. High-density lipoprotein (HDL) functionalities of engineered lipoprotein 2 (eLP2) in human umbilical vein endothelial cells (HUVECs). A) Reverse transcription–polymerase chain reaction analysis of lipopolysaccharide (LPS)-induced interleukin (IL)−1B mRNA expression to assess the anti-inflammatory activity. Data are presented as the mean ± standard deviation (N ≥ 4). B) Fluorescence-activated cell sorter (FACS) analysis of tumor necrosis factor-α–induced vascular cell adhesion molecule-1 (VCAM-1) expression to assess the anti-inflammatory activity. Cells were treated with samples at a concentration of 300 μg protein mL^{-1}. C) Quantitative analysis of the results obtained in (B). Data are presented as the relative mean fluorescence intensity ± standard deviation (N = 4). D) Confocal images of HUVECs in the vascular endothelial growth factor (VEGF)-induced tube formation assay. Cells were treated with samples at a concentration of 300 μg protein mL^{-1} (HDL samples) or 500 ng mL^{-1} (anti-VEGF antibodies). Bar, 1 mm. E) Tube area (left) and length (right) values based on the results obtained in (D). Data are presented as the relative mean fluorescence intensity ± standard deviation (N = 6).

consistent with the results of reverse transcription–polymerase chain reaction (RT–PCR) of extremely weak CD13 mRNA in THP-1 macrophages (Figure S5, Supporting Information). These results in HUVECs and THP-1 cells clearly demonstrated that the PEN and NGR peptide fusion increased HDL functionalities in most cases as well as the cell binding/uptake of rHDL, without inducing any significant cytotoxicity (Figure S3, Supporting Information).

3. Discussion

This study was inspired by our previous finding that the eLP1 eye-drop formulation is therapeutically active in CNV mice.[8] This finding was based on the following factors: i) ectopic utilization of a serum component (HDL) because of its functionalities that counteract some AMD pathologies and ii) the eye-surface absorption enhancement of eLP1 by attaching CPPs to HDL. Therefore, in this study, we focused on increasing the therapeutic efficacy of eLP1 by adding CNV-targeting capability. This strategy was successful to a great extent (Figure 1) and was mainly attributed to the unprecedented function of the NGR peptide, which is an absorption enhancer in mouse cornea (Figure 2) and does not cause significant cytotoxicities (Figure S3, Supporting Information). Another effort was made to evaluate the HDL functionalities of genetically-engineered HDL nanoparticles (eLP1 and eLP2) for the first time, and both PEN and NGR peptides in eLPs were found to be beneficial to HDL functionalities in a cell binding/uptake-dependent manner (Figures 4C,5, and 6). These HDL functionalities would be beneficial in CNV mice and clinical AMD.[5,13]

Active and safe absorption enhancers for the eye surface are gaining increasing attention for the development of eye drops.[2a,3] CPPs are a potential candidate, and one of the CPPs, known as the PEN peptide, was used in this study. To the best of our

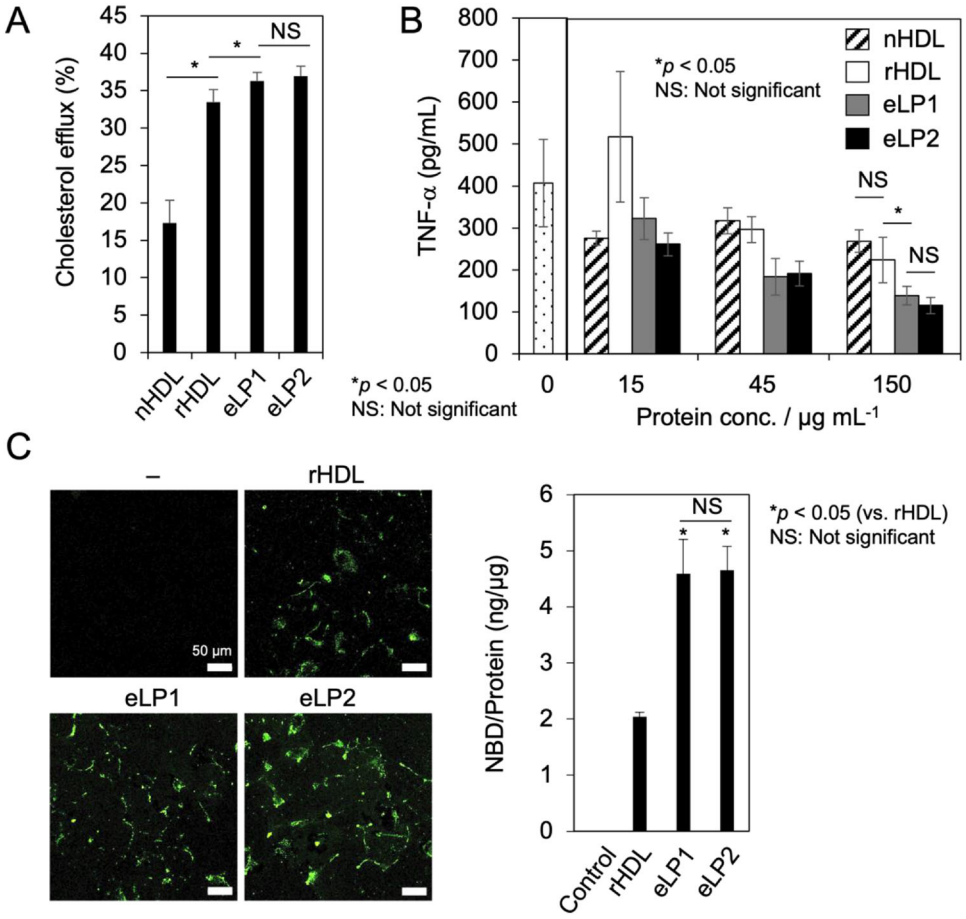

Figure 6. High-density lipoprotein (HDL) functionalities of engineered lipoprotein 2 (eLP2) in human monocyte (THP-1)-derived macrophages. A) Cholesterol-efflux capacity. Data are presented as the mean ± standard deviation (N ≥ 6). B) Enzyme-linked immunosorbent assay (ELISA) analysis of lipopolysaccharide-induced tumor necrosis factor (TNF)-α secretion to assess the anti-inflammatory activity. Data are presented as the mean ± standard deviation (N = 4). C) Confocal analysis of cell binding and uptake results (left, images; right, quantitative analysis). Cells were treated for 4 h with PBS, 1,2-dipalmitoyl-*sn*-glycero-3-phosphoethanolamine-*N*-(7-nitro-2-1,3-benzoxadiazol-4-yl) ammonium salt (NBD)-labeled reconstituted HDL lacking penetratin and NGR peptides (rHDL), engineered lipoprotein 1 (eLP1), or engineered lipoprotein 2 (eLP2) (1.5 μM NBD). Data are presented as the mean fluorescence intensity ± standard deviation (N = 4). Bar, 50 μm.

knowledge, no studies have reported for the utilization of eye-surface receptor ligands as enhancers. The migration pathway of eLP2 from the eye surface to the posterior choroid containing CNV sites was not fully addressed in this study; however, the more rapid binding of eLP2 in HCE-T cells than in Chang conjunctiva cells (Figure 4A,B, white bars) and the greater cargo accumulation (per area) in the retinal inner layer than in the CNV and choroid (Figure S4B,D,E, black bar, Supporting Information) suggest that the therapeutic efficacy of eLP2 in the posterior segment depends more on some local routes through the cornea than on a systemic route. Thus, our next challenge is to elucidate the detailed route of the transmission.

In CNV mice, the maximum efficacy of eLP2 was achieved at a dose of 0.6–0.85 μg protein/eye drops twice daily for 1 week (Figure 1C). This potency appears to be comparable to that of a single intravitreal injection of anti-VEGF antibody (0.4 μg) or anti-VEGF antibody (1.8 μg)/5[6]-carboxyfluorescein-labeled hexaarginine peptide (25 μg) eye drops (twice daily for 10 days).[14] In the current study, eLP2 could directly inhibit the tube formation of HUVECs to a greater extent than nHDL, although at a concentration much higher than that of anti-VEGFR antibodies (Figure 5D,E). Considering that the pathogenesis of laser-induced CNV is an acute inflammation after traumatic injury, anti-inflammation-related activities of eLP2 could be the mechanism of action in CNV mice. Cholesterol efflux in macrophages is also a potential target for anti-angiogenesis in AMD.[13,15] We demonstrated that the cholesterol-efflux capacity in THP-1 macrophages was significantly higher for eLP2 than for rHDL and nHDL (Figure 6A). In endothelial cells, both anti-inflammation and cholesterol efflux are considered targets for inhibiting angiogenesis by HDL;[11] however, in this study, the anti-inflammatory activities of eLP1 and eLP2 were comparable (Figure 5A–C). Considering these findings, the dramatic improvement in the therapeutic activity of eLP1 by NGR peptide fusion can be mainly attributed to its better corneal/conjunctival absorption (Figure 2) followed by CNV targeting (Figure S4A and B, Supporting Information) as well as enhanced tube formation inhibition (Figure 5D,E).

In this study, the biological activities of HDL variants were evaluated for the first time. Regarding anti-inflammatory activities, eLP1 and eLP2 showed significant favorable effects of PEN peptide fusion on LPS-treated HUVECs (Figure 5A) and LPS-treated THP-1 macrophages (Figure 6B). These effects can be attributed to the intrinsic anti-inflammatory activity of the PEN peptide.[12,16] This activity was more augmented by the fusion of the PEN peptide to rHDL than by their simple mixture (Figure S6B, Supporting Information). As both rHDL and the PEN peptide are amphiphilic, LPS (also amphiphilic) is assumed to be neutralized more efficiently by their complex (eLP1) than by their physical mixture. The effect of the functional peptide fusion was weaker in TNF-α-treated HUVECs than in LPS-treated HUVECs (Figure 5C), supporting the abovementioned assumption.

Additionally, rHDL bearing only an apoA-I fragment showed 1.5-fold higher cholesterol-efflux capacity in THP-1 macrophages than native HDL, and the genetic fusion of PEN peptide and the fragment was beneficial for further augmentation. Enhancement of endocytosis followed by recycling of eLP1 and eLP2 is considered a possible mechanism because the endocytosis of HDL facilitated its cholesterol efflux in THP-1 macrophages.[17] Thus, the PEN peptide could enhance the endocytosis of rHDL (Figure 6C).

The cholesterol-efflux capacity of HDL is affected by several other factors, such as the size and structures of its phospholipids, which determine the cholesterol affinity (unsaturated lipids < saturated lipids), and lipid membrane phase, which determines the cholesterol insertion capability (gel < liquid crystalline).[18] The size of (≈15 nm) and phospholipids used in (DSPC, phase-transition temperature of 55° C) eLP1 and eLP2 were selected based on the efficiency of the cargo (coumarin 6) delivery to the mouse posterior-eye segment, which may be disadvantageous for maximizing the cholesterol-efflux capacity. In contrast, our results revealed that the genetic engineering of apoA-I with the PEN peptide was an effective strategy for increasing the cholesterol-efflux capacity of rHDL.

4. Conclusion

We developed an HDL-based eye drop. The eye-drop instillation containing engineered HDL with two peptides, namely, PEN and NGR, effectively improved its therapeutic activity in an AMD mouse model. Consequently, the efficacy of the instillation of eLP2 eye drops (twice daily for 1 week) was comparable to that of a single intravitreal injection of anti-VEGF antibody in mice. Unexpectedly, the NGR peptide was also shown to be a novel corneal absorption enhancer in mice. Both peptides in eLP2 exerted beneficial effects of anti-inflammatory activity, cholesterol-efflux capacity, and antiangiogenic activity on HDL functionalities. Our results demonstrated that HDL engineering can expand the clinical application of HDL.

5. Experimental Section

Materials: Fluorescein isothiocyanate (FITC)-labeled anti-human CD13 antibody (WM-15), BCA protein assay kit, TrypLE Express, and SuperScript VILO Master Mix were purchased from Thermo Fisher Scientific, Inc. (Waltham, USA) (SuperScript VILO Master Mix is a trademark of Invitrogen). Heparin, phospholipids C assay kit, Dulbecco's phosphate-buffered saline (DPBS, pH 7.1–7.7), and TNF-α were obtained from FUJIFILM Wako Pure Chemical Corporation (Osaka, Japan). Benzalkonium chloride (BAC) was purchased from Nacalai Tesque, Inc. (Kyoto, Japan). Spectra/Por dialysis membrane (molecular weight cutoff [MWCO], 50 kDa) was purchased from Repligen Corp. (Waltham, USA). DC protein assay kit and anti-mouse CD13 monoclonal antibody (R3-63) were purchased from Bio-Rad Laboratories (Hercules, USA). Further, 1,2-dipalmitoyl-*sn*-glycero-3-phosphoethanolamine-*N*-(7-nitro-2-1,3-benzoxadiazol-4-yl) ammonium salt (NBD) was purchased from Avanti Polar Lipids, Inc. (Alabaster, AL, USA). LPS was purchased from AdipoGen Life Sciences (San Diego, CA, USA). nHDL was purchased from Lee Biosolutions (Maryland Heights, MO, USA). Recombinant human VEGF165 and anti-VEGF receptor antibodies (human VEGFR1/Flt1 Fc Chimera and human VEGFR2/KDR/Flk-1) were purchased from Bio-Techne (Minnesota, MN, USA). Moreover, DSPC was purchased from YUKA SANGYO CO., LTD.

General Procedures: Protein concentrations in rHDL and eLPs were determined using the Lowry method via DC protein assay kit, whereas phospholipid concentrations were determined using the enzymatic method based on choline oxidase as well as the *N*-ethyl-*N*-(2-hydroxy-3-sulfopropyl)−3,5-domethoxyaniline method with phospholipid C.[8] The hydrodynamic diameters of rHDL and eLPs in PBS (pH 7.4) were determined using Nanotrac UPA-UT151 particle-size analyzer (MicrotracBEL Corp., Osaka, Japan). Zeta-potential measurements of rHDL and eLPs were performed in 20 mM tris(hydroxymethyl)aminomethane (Tris)·HCl containing 10 v/v% PBS (pH 7.4) using Zetasizer Nano Z (Malvern Instruments, Malvern, UK). Cellular protein level was quantified using BCA protein assay kit according to the manufacturer's protocol.

cDNA Construction and apoA-I Variant Preparation: cDNAs expressing the N-terminal deletion variants of human apoA-I with or without the PEN peptide were prepared as described in the previous reports.[8,19] cDNA construction for the expression of a novel human apoA-I variant bearing NGR motif (CNGRCGG) at the N-terminus and PEN peptide at the C-terminus was performed as follows: a target apoA-I sequence was amplified with the following primers and inserted into the *KpnI* and *XbaI* sites of the pCOLD I bacterial expression vector (TaKaRa Bio, Inc., Shiga, Japan) to obtain N-terminal fusion:

Forward primer: 5′-ATGGTACCTGCAACGGCCGCTGCGGCGGCCTA AAGCTCCTTGACAACTGGGA-3′

Reverse primer (pCOLD vector sequence): 5′-GGCAGGGATCT TAGATTCTG-3′

The apoA-I variants were expressed in BL21(DE3) (Novagen, Madison, WI, USA) according to the manufacturer's protocol and were purified using Ni Sepharose High-Performance resin (Cytiva, Tokyo, Japan) packed in a Tricorn 10/100 column in the ÄKTAstart chromatography system (Cytiva) under denaturation conditions. Detailed protocols had been described previously.[20]

eLP Preparation and Characterization: It was prepared eLPs and rHDL following the previously reported method,[8] and eLP2 was prepared similarly as eLP1, with minor modifications. Briefly, dialysis after reaction was performed overnight against 3 L of PBS using the dialysis membrane (MWCO, 50 kDa) to remove urea and sodium cholate. The starting temperature of PBS was 55 °C (phase-transition temperature of DSPC), which was reduced to room temperature during dialysis. For fluorescence labeling, 0.5 mol% ethanol-solubilized coumarin-6 or 1 mol% NBD was added to DSPC, followed by evaporation to obtain lipid films. The subsequent procedures have been described above.

AFM Analysis: eLP2 (5 μg protein/mL in PBS) was applied to a mica surface for 4 min, and floating samples were rinsed out with deionized water. Images were acquired in deionized water to maintain the samples tightly fixed on the mica surface. Image acquisition was performed using SPM-9700HT (Shimadzu Corporation, Kyoto, Japan) equipped with a cantilever BL-AC40TS (Olympus Corporation, Tokyo, Japan) with a spring constant of 0.04–0.08 N/m and resonant frequency of 81.1–114.4 kHz. The scanning rate was 3.5 frames/s.

CD: Chirascan V100 (TEGA Science, Inc., Chiba, Japan) was used to record far-ultraviolet CD spectra from 200 to 260 nm at room temperature under nitrogen atmosphere. The CD spectra of rHDL and eLPs in PBS were

measured at a dose of 50 μg protein/mL, and the obtained values were corrected by subtracting the PBS baseline. Percent helix was estimated via a previously reported method.[21]

Cell Culture: HUVECs and the culture medium EGM2 were obtained from PromoCell (Heidelberg, Germany). The medium was supplemented with 2 v/v% fetal bovine serum (FBS; Japan Bio Serum, Hiroshima, Japan) and 1 v/v% antibiotic–antimycotic stock solution. The cells were seeded onto culture dishes (BD, Franklin Lakes, NJ, USA) coated with 0.5 w/v% gelatin (Nacalai Tesque, Inc.). HCE-T cells were purchased from RIKEN Cell Bank (Ibaraki, Japan) and maintained in Dulbecco's modified Eagle medium/Ham's nutrient mixture F12 (DMEM/Ham's F12; Thermo Fisher Scientific, Inc.) supplemented with 10 v/v% FBS, 5 μg mL^{-1} recombinant human insulin, 10 ng mL^{-1} recombinant human epithelial growth factor, and 0.5 v/v% dimethyl sulfoxide. Chang conjunctiva cells (clone 1–5c-4) were obtained from American Type Culture Collection (ATCC; Manassas, VA, USA) and maintained in Medium 199 (Thermo Fisher Scientific, Inc.) supplemented with 10 v/v% FBS. Immortalized ARPE-19 cells were purchased from ATCC and maintained in DMEM/Ham's F12 (Nacalai Tesque, Inc.) supplemented with 10 v/v% FBS. Human monocytic leukemia (THP-1) cells were obtained from Cell Resource Center for Biomedical Research Institute of Development, Aging and Cancer Tohoku University. THP-1 cells were maintained in RPMI1640 (FUJIFILM Wako Pure Chemical Corporation) supplemented with 10 v/v% FBS and 2 mM L-glutamine (Nacalai Tesque, Inc.). All cells were maintained under 5 v/v% CO_2 at 37° C, and the culture medium was replaced with fresh medium every 2 days. Subculturing of THP-1 cells was performed only by replacement of the medium; the cells were treated with phorbol 12-myristate 13-acetate (Merck KGaA, Darmstadt, Germany) for ≥48 h to obtain macrophage-like cells. Other cells were subcultured after treatment with 2.5 g L^{-1} trypsin/1 mmol L^{-1} ethylenediamine-*N,N,N",N"*-tetraacetic acid solution (Nacalai Tesque, Inc.).

Cytotoxicity Assay: Cells were treated with eLP2 for 22 h (HUVECs) and 15 or 60 min (HCE-T and Chang conjunctiva cells) in their respective cell culture media, as mentioned previously. The WST-8 assay was performed using Cell Counting Kit-8 (Dojindo Laboratories, Kumamoto, Japan). Lactate dehydrogenase (LDH) release was measured via Cytotoxicity LDH Assay Kit-WST (Dojindo Laboratories). BAC was used as a positive control. These assays were performed according to their manufacturers' protocols. The transepithelial electrical resistance (TEER) assay using HCE-T and Chang conjunctiva cells was performed using ad-MED Vitrigel (Kanto Kagaku, Tokyo, Japan) based on the Vitrigel-eye irritancy test method.[22] For Chang conjunctiva cells, monolayer culturing was performed according to a previous report.[23] Each sample was added to HCE-T or Chang conjunctiva cell monolayer at a concentration of 400 μg protein/mL. TEER measurement was performed using Millicell ERS-2 Voltohmmeter (Millicell is a trademark of Merck KGaA). Experiments were performed in duplicate and repeated 4 times.

Flow Cytometry: HUVECs were seeded into a 12-well plate at a density of 2×10^5 cells mL^{-1} and then incubated at 37° C for 6 h. The attached cells were treated with 300 μg protein/mL nHDL, rHDL, and eLPs for 16 h at 37° C. The cells were stimulated with 1 ng mL^{-1} TNF-α for 4 h and then washed with DPBS. HCE-T or Chang conjunctiva cells were seeded into a 12-well plate at a density of 2×10^5 cells mL^{-1} and then incubated overnight at 37° C. The cells were scraped off after treatment with DPBS containing 2.5 v/v% FBS. Subsequently, the cells were incubated for 20 min on ice with FITC-labeled anti-CD13 antibody WM-15 or PE mouse anti-human VCAM-1/CD106 antibody Clone 51-10C9 (RUO) (BD Biosciences, Franklin Lakes, NJ, USA). BD FACSCanto II (BD FACSCantoTM II is a trademark of BD Biosciences) flow cytometer was used to analyze ≥10000 cells per sample.

Quantitative Reverse Transcription–Polymerase Chain Reaction (qRT–PCR): Total RNA was isolated from cells using ISOGEN II (Nippon Gene Co., Ltd., Tokyo, Japan). To obtain cDNA, RNA was reverse-transcribed using SuperScript VILO Master Mix. Then, real-time PCR was performed using a master mix (TB Green Premix Ex TaqII [Tli RNaseH Plus], TaKaRa Bio, Inc.) and Thermal Cycler Dice Real Time System (TaKaRa Bio, Inc.). Individual samples were used in duplicate, and each experiment was repeated at least 4 times. The $2^{-\Delta\Delta Ct}$ method was used to analyze the relative changes in gene expression. β-actin *(ACTB)* or glyceraldehyde-3-phosphate dehydrogenase (*GAPDH*) was used as an endogenous normalization control. Primer sequences are listed in Table S1 (Supporting Information).

Cellular Uptake of rHDL and eLPs: To analyze the cellular uptake of eLPs, 1×10^4 cells were seeded onto a triple-well glass-bottom dish (AGC Techno Glass Co., Ltd., Chiba, Japan) containing 100 μL of the culture medium and incubated overnight. The cells were washed with DPBS and then incubated at 37° C with NBD-labeled rHDL or eLPs (1.5 μM NBD) in a culture medium without heparin. Next, the medium was removed, and the cells were washed twice with DPBS supplemented with heparin (40 U mL^{-1}). Finally, the cells were observed via confocal laser scanning microscopy (CLSM) using LSM 800 (Carl Zeiss, Jena, Germany), and image analyses were performed using ZEISS ZEN analysis software. For quantitative analysis, the cells were scraped off after treatment with DPBS. The cells were lysed with RIPA buffer (5 mM Tris-HCl [pH 7.6], 0.02 w/v% sodium dodecyl sulfate, 0.18 w/v% NaCl, 0.2 w/v% Nonidet P-40, and 0.2 w/v% sodium deoxycholate) by performing the freeze–thaw cycle twice (−80° C, 20 min; 37° C, 20 min). Cell lysates were prefrozen at −80° C before freeze–drying (FDS-1000; Tokyo Rikakikai Co., Ltd., Tokyo, Japan). TECAN INFINITE M PLEX (Tecan Japan Co., Ltd., Kanagawa, Japan) was used to determine the NBD concentration.

Evaluation of HDL Functionalities: TNF-α secretion was analyzed using enzyme-linked immunosorbent assay (ELISA) via a commercially available ELISA kit (R&D Systems, Inc., Minneapolis, MN, USA). Briefly, THP-1 macrophages (1×10^5 cells) were treated with each sample (rHDL, eLP1, and eLP2; 0–300 μg protein/mL) for 24 h. Then, 100 μL of the culture supernatant was added to each well of a capture antibody-coated 96-well plate (AGC Techno Glass Co., Ltd.). TNF-α concentration was determined according to the manufacturer's protocol, except for antibody dilution (capture antibody, 1:240; detection antibody, 1:120). IL1B mRNA and VCAM-1 protein expression was evaluated using qRT–PCR and flow cytometry, respectively, as mentioned previously. HUVECs pretreated with 0–150 μg protein/mL rHDL or eLPs for 16 h were treated with LPS (10 ng mL^{-1}, 6 h) or TNF-α (1 ng mL^{-1}, 4 h) before assessing IL1B mRNA or VCAM-1 protein expression.

To determine the cholesterol-efflux capacity, THP-1 macrophages (1×10^6 cells mL^{-1}) were treated with 0.6 μCi/mL^{-1} [^{3}H]-cholesterol for 24 h. After washing with PBS, the cells were treated with nHDL, rHDL, or eLPs at a concentration of 50 μg protein/mL for 4 h. Subsequently, the radioactivity of [^{3}H] was estimated via liquid scintillation counting (PerkinElmer Inc., Waltham, MA, USA). All steps were performed in the presence of 2 μg mL^{-1} acyl-coenzyme A and cholesterol acyltransferase inhibitor Sandoz 58-035 (Merck KGaA).

For the HUVEC tube formation assay, HUVECs were seeded into a 12-well plate at a density of 3×10^4 cells mL^{-1} and then incubated for 6 h at 37° C. The attached cells were treated for 24 h with 300 μg protein/mL rHDL, 300 μg protein/mL eLPs, or 500 ng protein/mL antibodies (anti-VEGFR1, 2) in the presence of 25 ng mL^{-1} VEGF165 (Bio-Techne). Subsequently, the cells were trypsinized and centrifuged (300 ×*g*, 24° C, 3 min). The cells were resuspended with the culture medium containing 2 v/v% FBS and then transferred to a PhenoPlate-96 (PerkinElmer Inc.) coated with growth factor-reduced Matrigel Matrix (Matrigel Matrix is a trademark of BD Biosciences). Operetta CLS High Content Analysis System (Operetta CLSTM High Content Analysis System is a trademark of PerkinElmer Inc.) was used to assess the tubulogenesis of HUVECs stained with 1 μM Cellstain-Calcein-AM solution (Cellstrain-Calcein-AM solution is a trademark of Dojindo Laboratories). All experiments were performed in duplicate and repeated at least 4 times.

Mouse Strains: Animal experiments were performed in accordance with the Association for Research in Vision and Ophthalmology Statement for the Use of Animals in Ophthalmic and Vision Research and the Guideline for Animal Experiments of Kyoto University (MedKyo 22 261) and Animal Experiment Ethics Committee of Toyama Prefectural University (R4-8).

Evaluation of Binding to the Mouse Cornea: PBS or NBD (rHDL, eLP1, or eLP2; 1.5 μM)-labeled HDL-based eye drop was administered topically to the eye of male adult mice (weight: 20–25 g; C57BL6/J; Japan SLC, Shizuoka, Japan). A single dose (3 μL) of the sample was dropped

onto the corneal surface using a micropipette. The eyes were enucleated 30 min after topical administration, fixed at 4° C overnight with 4 w/v% paraformaldehyde (PFA) in PBS (Nacalai Tesque, Inc.), immersed in 20 w/v% sucrose at 4° C for 24 h, and then embedded into optical cutting temperature compound (Miles Laboratories, Elkhart, IN, USA). Overall, 25-µm thick cryostat sections were prepared using Leica CM1860 UV (Leica Microsystems, Wetzlar, Germany), mounted onto New Silane 3 glass slides (Muto Pure Chemicals, Co., Ltd., Tokyo, Japan), and preserved at −30° C until observation. Corneal images were obtained via CLSM using LSM 800 and fluorescence filters for NBD (ex./em. = 488/500–580 nm). Image J (National Institutes of Health, Bethesda, MD, USA) was used to evaluate the fluorescence intensities of NBD. The intensity data were obtained from the mean intensities of four slices per sample.

In Vivo CD13 Receptor Expression: Immunohistochemical analysis of mouse eyes was performed by Morphotechnology Co., Ltd. (Hokkaido, Japan). Enucleated eyes were fixed with 10 v/v% neutral-buffered formalin at room temperature for 48 h. The eyes were embedded into paraffin using Tissue-Tek VIP 6 AI (Tissue-Tek VIP is a trademark of Sakura Finetek Japan Co., Ltd., Tokyo, Japan). Then, 4-µm paraffin slices of mouse eyes were prepared using Retoratome REM-710 (Yamato Kohki Industrial Co., Ltd., Saitama, Japan). After deparaffinization, each slice was washed with deionized water, followed by antigen retrieval using Target Retrieval Solution High pH (Agilent Technologies, Inc., Santa Clara, CA, USA) at 95° C for 20 min. The samples were cooled down to room temperature for 20 min and washed with deionized water. For blocking of endogenous peroxidase, samples were treated with 0.3 v/v% hydrogen peroxide solution for 10 min, washed with Tris-buffered saline (TBS), incubated at 4° C overnight with anti-mouse CD13 monoclonal antibody (R3-63, 1:100), washed with TBS twice, incubated with biotinylated anti-rat immunoglobulin G (IgG; 1:200; Vector Laboratories, Inc., Stuttgart, Germany) at room temperature for 30 min, washed with TBS twice, and subjected to the avidin/biotin/horseradish peroxidase system (Vectastain Elite ABC Standard Kit [Vector Laboratories, Inc.]) using 3,3′-diaminobenzidine as a substrate (Nichirei Corporation, Tokyo, Japan). Further, the samples were treated with hematoxylin solution, washed with deionized water, treated with serially diluted ethanol (70, 95, and 100 v/v%), and finally treated with xylene solution. Observation was performed using NanoZoomer S210 virtual slide scanner (Hamamatsu Photonics K.K., Shizuoka, Japan).

In Vivo Study in Mouse with Laser-Induced CNV: CNV induction was performed according to the previous report.[8] The mice received eye drops twice daily for 1 week. Then, the eyes were enucleated, fixed with 4 w/v% PFA in PBS for ≥20 min on ice, and sectioned at the limbus. The cornea, iris, and lens were excised to prepare an eyecup. For CNV quantification, retinal pigment epithelium/choroidal flat mounts were stained with rat anti-CD102 antibody (1:200, BD Biosciences) and Alexa 488-conjugated anti-rat IgG (1:500, Thermo Fisher Scientific, Inc.) as the primary and secondary antibodies, respectively, after treatment with 5 w/v% Block Ace Powder (Block Ace Powder is a trademark of KAC Co., Ltd., Kyoto, Japan) in PBS containing 0.5 w/v% Triton-X for 1 h. Images were obtained via CLSM (LSM 5 Pascal, Carl Zeiss).

For the CNV-targeting analysis, coumarin 6-loaded samples were prepared according to the previous report.[8] The mice received eye drops (100 µM coumarin 6) once; after 30 min, the eyes were enucleated and treated as described above.

Statistical Analysis: Differences in mean values between more than two groups were determined using one-way analysis of variance and post-hoc Tukey–Kramer correction. For all statistical analyses, p-values of <0.05 were considered to indicate statistical significance. Data are presented as mean values ± standard deviation in graphs.

Supporting Information

Supporting Information is available from the Wiley Online Library or from the author.

Acknowledgements

Theauthors thank Hitomi Suetsugu for technical assistance in animal experiments and Akiko Soto for technical assistance with protein expression and purification. This study was supported by JSPS KAKENHI Grant Number JP20K18378 [K.S.], JP18K18460 [T.M.], and JP21H03821 [T.M.].

Conflict of Interest

M.O. has received honoraria from Amgen and Kowa outside the submitted work. A.T. has received financial support from Canon, Findex, and Santen outside the submitted work. R.F., S.K., K.S., A.T., and T.M. have applied the technology of eye drop therapy in this paper for a patent (P2021-138629A). All other authors declare no conflict of interest.

Data Availability Statement

The data that support the findings of this study are available from the corresponding author upon reasonable request.

Keywords

absorption enhancer, age-related macular degeneration, antiangiogenic activity, anti-inflammatory activity, high-density lipoproteins, neovasculature-targeting

Received: May 31, 2023
Revised: July 31, 2023
Published online: August 25, 2023

[1] N. H. Bennett, H. R. Chinnery, L. E. Downie, L. J. Hill, L. M. Grover, *Adv. Funct. Mater.* **2020**, *30*, 1908476.
[2] a) R. V. Moiseev, P. W. J. Morrison, F. Steele, V. V. Khutoryanskiy, *Pharmaceutics* **2019**, *11*, 321; b) S. Bonengel, A. Bernkop-Schnurch, *J. Controlled Release* **2014**, *195*, 120.
[3] a) S. Pescina, C. Ostacolo, I. M. Gomez-Monterrey, M. Sala, A. Bertamino, F. Sonvico, C. Padula, P. Santi, A. Bianchera, S. Nicoli, *J. Controlled Release* **2018**, *284*, 84; b) A. Thareja, H. Hughes, C. Alvarez-Lorenzo, J. J. Hakkarainen, Z. Ahmed, *Pharmaceutics* **2021**, *13*, 276.
[4] R. S. Apte, *N. Engl. J. Med.* **2021**, *385*, 539.
[5] M. Fleckenstein, T. D. L. Keenan, R. H. Guymer, U. Chakravarthy, S. Schmitz-Valckenberg, C. C. Klaver, W. T. Wong, E. Y. Chew, *Nat. Rev. Dis. Primers* **2021**, *7*, 31.
[6] A. Rohatgi, M. Westerterp, A. von Eckardstein, A. Remaley, K. A. Rye, *Circulation* **2021**, *143*, 2293.
[7] K. B. Uribe, A. Benito-Vicente, C. Martin, F. Blanco-Vaca, N. Rotllan, *Biomater. Sci.* **2021**, *9*, 3185.
[8] K. Suda, T. Murakami, N. Gotoh, R. Fukuda, Y. Hashida, M. Hashida, A. Tsujikawa, N. Yoshimura, *J. Controlled Release* **2017**, *266*, 301.
[9] H. M. Ellerby, W. Arap, L. M. Ellerby, R. Kain, R. Andrusiak, G. Del Rio, S. Krajewski, C. R. Lombardo, R. Rao, E. Ruoslahti, D. E. Bredesen, R. Pasqualini, *Nat. Med.* **1999**, *5*, 1032.
[10] F. Curnis, G. Arrigoni, A. Sacchi, L. Fischetti, W. Arap, R. Pasqualini, A. Corti, *Cancer Res.* **2002**, *62*, 867.
[11] J. T. Tan, M. K. Ng, C. A. Bursill, *Cardiovasc. Res.* **2015**, *106*, 184.
[12] M. Fotin-Mleczek, S. Welte, O. Mader, F. Duchardt, R. Fischer, H. Hufnagel, P. Scheurich, R. Brock, *J. Cell Sci.* **2005**, *118*, 3339.
[13] L. Zhu, M. Parker, N. Enemchukwu, M. Shen, G. Zhang, Q. Yan, J. T. Handa, L. Fang, Y. Fu, *Commun Biol* **2020**, *3*, 386.

[14] F. de Cogan, L. J. Hill, A. Lynch, P. J. Morgan-Warren, J. Lechner, M. R. Berwick, A. F. A. Peacock, M. Chen, R. A. H. Scott, H. Xu, A. Logan, *Invest. Ophthalmol. Visual Sci.* **2017**, *58*, 2578.

[15] a) L. Fang, S. H. Choi, J. S. Baek, C. Liu, F. Almazan, F. Ulrich, P. Wiesner, A. Taleb, E. Deer, J. Pattison, J. Torres-Vazquez, A. C. Li, Y. I. Miller, *Nature* **2013**, *498*, 118; b) A. Sene, A. A. Khan, D. Cox, R. E. Nakamura, A. Santeford, B. M. Kim, R. Sidhu, M. D. Onken, J. W. Harbour, S. Hagbi-Levi, I. Chowers, P. A. Edwards, A. Baldan, J. S. Parks, D. S. Ory, R. S. Apte, *Cell Metab.* **2013**, *17*, 549.

[16] a) T. Letoha, E. Kusz, G. Papai, A. Szabolcs, J. Kaszaki, I. Varga, T. Takacs, B. Penke, E. Duda, *Mol. Pharmacol.* **2006**, *69*, 2027; b) R. Chaby, *Cell. Mol. Life Sci.* **2004**, *61*, 1697.

[17] T. A. Pagler, S. Rhode, A. Neuhofer, H. Laggner, W. Strobl, C. Hinterndorfer, I. Volf, M. Pavelka, E. R. Eckhardt, D. R. van der Westhuyzen, G. J. Schutz, H. Stangl, *J. Biol. Chem.* **2006**, *281*, 11193.

[18] a) X. M. Du, M. J. Kim, L. Hou, W. L.e Goff, M. J. Chapman, M. Van Eck, L. K. Curtiss, J. R. Burnett, S. P. Cartland, C. M. Quinn, M. Kockx, A. Kontush, K. A. Rye, L. Kritharides, W. Jessup, *Circ. Res.* **2015**, *116*, 1133; b) W. S. Davidson, K. L. Gillotte, S. Lund-Katz, W. J. Johnson, G. H. Rothblat, M. C. Phillips, *J. Biol. Chem.* **1995**, *270*, 5882; c) B. Ramstedt, J. P. Solotte, *Biophys. J.* **1999**, *76*, 908.

[19] T. Murakami, W. Wijagkanalan, M. Hashida, K. Tsuchida, *Nanomedicine (London, U. K.)* **2010**, *5*, 867.

[20] R. Fukuda, M. Saito, S. Shibukawa, A. Sumino, M. Nakano, T. Murakami, *Biochemistry* **2020**, *59*, 1455.

[21] Y. H. Chen, J. T. Yang, *Biochem. Biophys. Res. Commun.* **1971**, *44*, 1285.

[22] H. Yamaguchi, H. Kojima, T. Takezawa, *Toxicol. Sci.* **2013**, *135*, 347.

[23] G. M. Yanochko, S. Khoh-Reiter, M. G. Evans, B. A. Jessen, *Toxicol. In Vitro* **2010**, *24*, 1324.